Supporting information

Pd/CNT with controllable Pd particle size and hydrophilicity for improved direct synthesis efficiency of H_2O_2

Huan You[a], Chengbing Fu[a], Meng Wang[a], Chunliang Yang[a], Yongyong Shi[a], Hongyan Pan[a,b,c]*, Qian Lin[a]*

*Corresponding authors

a. Department of Chemical Engineering, School of Chemistry and Chemical Engineering, Guizhou University, and Guizhou Key Laboratory for Green Chemical and Clean Energy Technology, Guiyang, Guizhou 550025, China

b. Guizhou phosphating group liability co. LTD, Guiyang 550005,China

c. State key laboratory of efficient utilization for low grade phosphate rock and its associated resources, Guiyang, Guizhou 550005,China

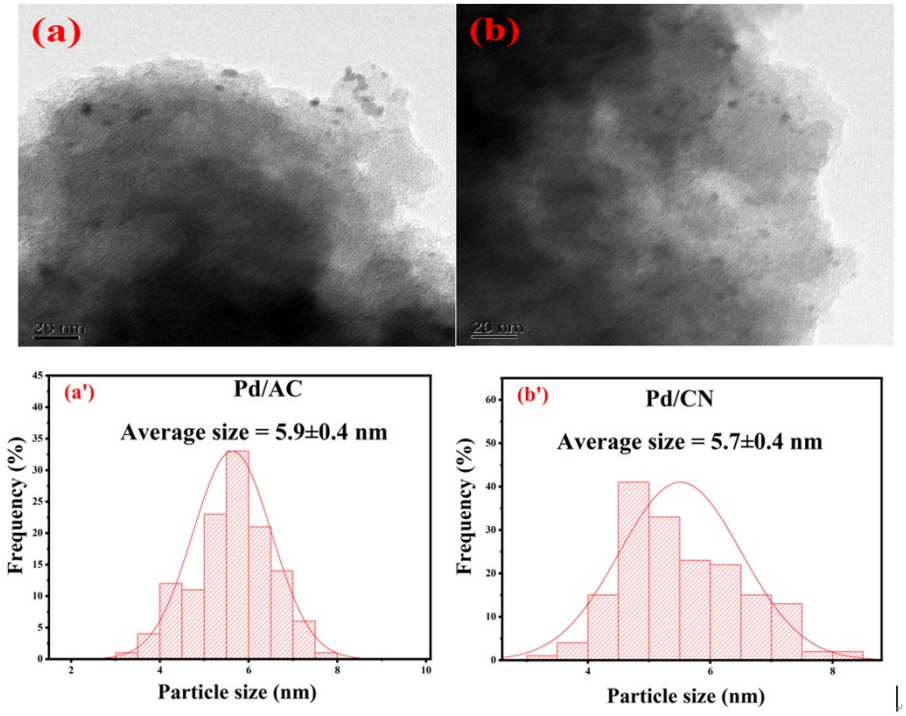

Fig. S1 TEM images and particle size statistics of the catalysts. (a, a') Pd/AC; (b, b') Pd/CN.

For comparison, these two catalysts in the Fig.S1 above is supported by AC and CN (nitrogen doped in AC).

Tab. S1 The particle size of catalyst calculated by Scherrer formula

Sample	Pd /CNT	Pd /CNT-N	Pd /CNT-OB	Pd /CNT-OB-N	Pd /CNT-OA	Pd /CNT-OA-N
Partical size(nm)	6.2	5.4	4.6	4.4	4.0	3.9

Tab. S2 Pd^0/Pd^{2+} ratio in catalysts.

Catalyst	Pd^0(%)	Pd^{2+}(%)	Pd^0/Pd^{2+}	Pd(%)
Pd/CNT	66.54	33.46	1.989	1.94%
Pd/CNT-N	69.23	30.77	2.250	1.96%
Pd/CNT-OB	67.77	32.23	2.103	1.97%
Pd/CNT-OB-N	72.59	27.41	2.648	1.98%
Pd/CNT-OA	66.59	33.41	1.993	1.95%
Pd/CNT-OA-N	70.93	29.07	2.440	1.96%

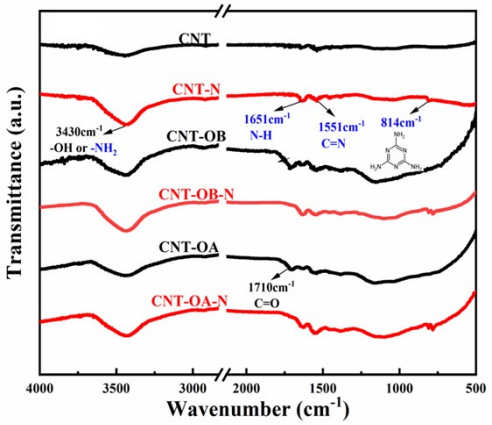

Fig. S2 FTIR spectrum analysis of carbon materials.

FTIR and XPS were used to characterize the surface properties of carbon materials, as shown in Fig. S2. After O dopped in CNT, a new C=O stretching vibration peak appears in CNT-OA，CNT-OA/N, CNT-OB, CNT-OB/N at 1710cm^{-1}. Compared with carbon material CNT (Fig. S2.), three new vibration peaks at 1651cm^{-1}, 1551cm^{-1} and 814cm^{-1} were observed on nitrogen-dopping samples CNT-N, CNT-OA-N and CNT-OB-N, respectively. Among them, the wavenumber of 1651cm^{-1} is attributed to the torsional vibration of the N-H bond in melamine; 1551cm^{-1} is the stretching vibration of C=N, and 814cm^{-1} is the deformation vibration of the triazine ring of melamine.

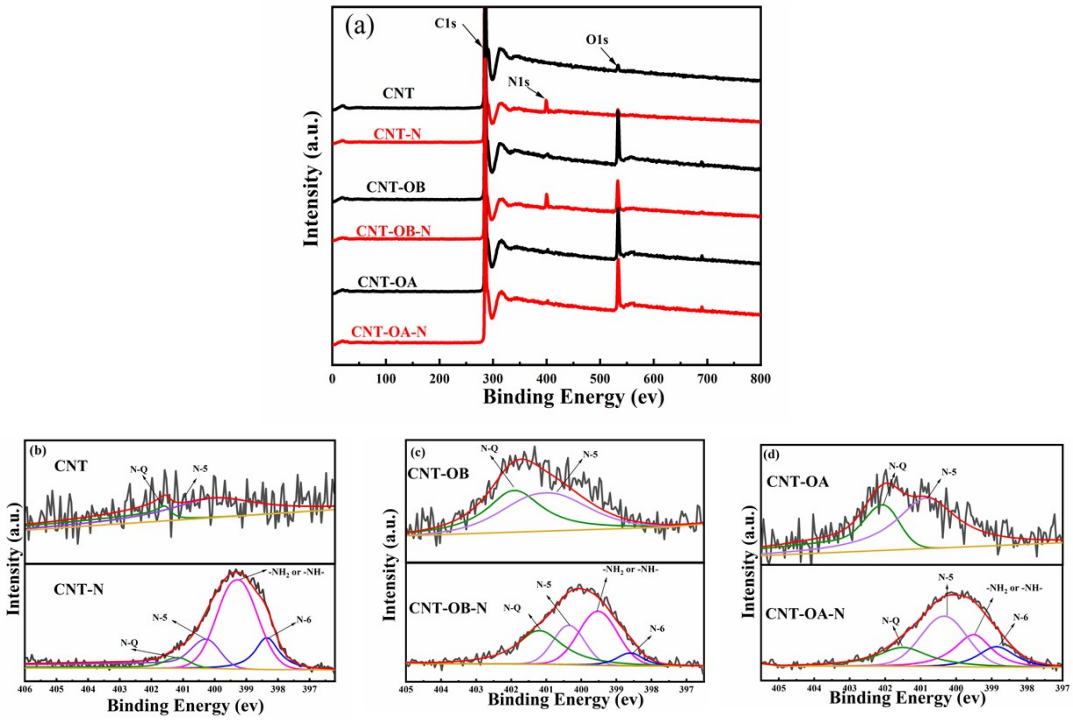

Fig. S3 XPS analysis of carbon materials; (a) XPS spectra; (b-d) N1s XPS spectra.

N1s XPS fine spectrum Fig. S3 (a) of carbon material was analyzed and shown in Fig. S3 (b-d). The binding energy peak at 398.3 eV can be classified as the signal of pyridine-like (N-6) nitrogen element, in which nitrogen atom binds to carbon atom in the form of SP^2 hybrid. The binding energy (BE) near 399.7eV could be assigned to -NH_2 or -NH-, while those BE near 400.5eV could be assigned to Pyrrolic nitrogen (N-5). The binding energy (BE) near 401.1-403.6 eV could be assigned to Quarternary nitrogen (N-Q). N1s peak of CNT can be fitted into two peaks which correspond to pyrrolic nitrogen (N-5) and quarternary nitrogen (N-Q). Compared to CNT, N1s binding energies of CNT-N, CNT-OB-N and CNT-OA-N shifted to the direction of lower binding energy and can be deconvoluted into four superimposed peaks, which corresponds to N-5, N-Q, pyridinic nitrogen (N-6) and Pyridinic-N-oxide (N-X)[1-3]. This indicated that N-6 and -NH_2 (or -NH-) were produced in the nitrogen-doped carbon material. Among them, pyridine nitrogen N-6 could increase the hydrophilicity of the material [4-5].

Tab. S3 Adsorption of H_2 and O_2 of catalysts.

Catalyst	H_2 adsorption (mmol/g)	O_2 non dissociative adsorption (mmol/g)	O_2 dissociation adsorption (mmol/g)
Pd/CNT	0.009	0.040	0.132
Pd/CNT-N	0.016	0.064	0.141
Pd/CNT-OB	0.033	0.073	0.174
Pd/CNT-OB-N	0.055	0.094	0.145
Pd/CNT-OA	0.045	0.070	0.169
Pd/CNT-OA-N	0.060	0.081	0.153
CNT	—	—	—

Tab. S4 Hydrophilicity test of carbon materials

Number	Sample	Contact Angle (°)	XPS				EA		
			C (%)	N (%)	O (%)	O+N (%)	C (%)	N (%)	O (%)
1	CNT	66.37°	98.54	0.41	1.05	1.46	97.41	0.35	2.24
2	CNT-N	43.61°	95.00	3.70	1.31	5.08	93.78	4.14	2.08
3	CNT-OB	31.84°	91.53	0.76	7.71	8.47	91.29	0.66	8.05
4	CNT-OB-N	21.39°	88.50	4.06	7.43	11.49	86.76	5.96	7.28
5	CNT-OA	34.38°	90.86	0.85	8.29	9.14	91.45	0.76	8.79
6	CNT-OA-N	26.71°	89.98	3.52	6.5	10.02	88.16	4.09	7.07

Surface chemical properties of carbon materials, such as hydrophilicity, polarity and proton affinity, determines its adsorption ability towards charged metal precursors in solution. Tab. S4 lists the contact angle of carbon materials. Compared with none-dopped CNT, nitrogen and oxygen modified CNT-N, CNT-OB, CNT-OA, CNT-OB-N and CNT-OA-N showed higher hydrophilicity in water, especially for CNT-OB-N catalyst which has the smallest contact angle (21.39°) indicating its best hydrophilicity among all samples because of the hydrogen bond formed between water molecules and the N-5 nitrogen on pyrrole and N-6 nitrogen on pyridine which doped to the CNT. For samples of CNT-OB, CNT-OA, CNT-OB-N and CNT-OA-N, their hydrophilicity was also increased indicating the effect of N, O doping, especially the N and O co-doping. Fig. S4 shows that C, N and O were detected on the prepared materials by XPS survey and EA of the samples, and the content of N and O in modified samples increased

significantly, especially for CNT-OB-N and CNT-OA-N.

Tab. S5 Catalytic performance of the reported Pd based catalysts for H_2O_2 direct synthesis

Catalyst	Pd(wt%)	Productivity ($mmol \cdot g_{Pd}^{-1} \cdot h^{-1}$)	H_2O_2 Sel.(%)	T(C°)/P(bar)/ Time(h)	Additives	Refs.
Pd/CNT-OB-N[a]	1.98	9943	91	0/1/1	1.8 ml H_2SO_4	This work
Pd/HHDMA/AC[b]	0.6	8400	80	0/40/0.5	-	[6]
Pd/AC[b]	1	6397	54	2/30/0.25	0.03 M H_2SO_4	[7]
Pd/CMK-3[c]	5	5600	-	5/20/1.5	0.04 M HCl	[8]
Pd/N-CNT[d]	0.9	1422	45	r.t/10/1.5	250 ml H_2SO_4	[9]
Pd/AC[b]	5	1040	42	2/40/0.5	-	[10]
Pd/N-CNT[d]	0.3	140	68	r.t/30/0.33	125 ml H_2SO_4	[11]
Pd/CB[e]	2.5	129	74	10/1/4	0.03 M HCl	[12]
Pd-Co@HCS	2	1996	87	0/1/1	0.9 ml H_2SO_4	[13]
Pd-Sn@hollow@C	2	3197	93	0/1/1	1.8 ml H_2SO_4	[14]
Pd-Au/C	2.5	6400	>98	2/4/0.5	2% HNO_3	[15]
Pd-Pt/O_5SZr	1.3	1236	70	20/1/12	0.03 M H_2SO_4	[16]

[a] multi-walled carbon nanotubes;

[b] activated carbon;

[c] Ordered mesoporous carbon;

[d] Carbon nanotubes;

[e] Carbon black.

References

1. Ferrero G A, Fuertes A B and Sevilla M, *Carbon*., 2016, **106**, 179–187.
2. Ghimbeu C M, Luchnikov V A, *Microporous Mesoporous Mater*,. 2018, **263**, 42–52.
3. Wang Y Y, Hou B H and Lü H Y, *RSC Advances*., 2015, **5**, 97427–97434.
4. Xiong W, Liu M and Gan L, *Colloid Surfaces A*., 2012, **411**, 34–39.
5. Farzin Nejad N, Shams E and Amini M K, *Fuller Nanotub Car N*., 2016, **24**, 786–795.
6. Ghedini E, Menegazzo F and Signoretto M, *J Catal*., 2010, **273**, 266-273.
7. S. Abate, R. Arrigo, M.E. Schuster, S. Perathoner, G. Centi, A. Villa, D. Su and R. Schlögl, *Catal. Today*., 2010, **157**, 280–285.
8. J.K. Edwards, B. Solsona, E. Ntainjua N, A.F. Carley, A.A. Herzing, C.J. Kiely and G.J. Hutchings, *Science*., 2009, **323**, 1037–1041.
9. G.M. Lari, B. Puértolas, M. Shahrokhi, N. López and J. Pérez-Ramírez, *Angew. Chemie -Int. Ed*., 2017, **56**, 1775–1779.
10. J. Gu, S. Wang, Z. He, Y. Han and J. Zhang, *Catal. Sci. Technol*., 2016, **6**, 809–817.
11. R. Arrigo, M.E. Schuster, S. Abate, G. Giorgianni, G. Centi, S. Perathoner,S. Wrabetz, V. Pfeifer, M. Antonietti and R. Schlögl, *ACS Catal*., 2016, **6**, 6959–6966.
12. B. Hu, W. Deng, R. Li, Q. Zhang, Y. Wang, F. Delplanque-Janssens, D. Paul, F. Desmedt and P. Miquel, *J. Catal*., 2014, **319**, 15–26.
13. Y Wang, Pan H and Lin Q, *Catalysts*,. 2020, **10**, 303.
14. Zhang J, Liu P and Shi Y, *New Journal of Chemistry*, 2021, **45**.
15. Jennifer, K and Edwards., *Science*, 2009.
16. Bernardotto G, F Menegazzo and F Pinna, *Applied Catalysis A General*., 2009, **358**, 129-135.